Cosmogenic and nucleosynthetic anomalies resolved in IVB meteorites using Palladium isotopes.

B. Mayer[1], M. Humayun[1] and N. Wittig[2]. [1]National High Magnetic Field Laboratory & Dept. of Earth,
Ocean & Atmospheric Science, Florida State University, Tallahassee, FL 32310, USA (mayer@magnet.fsu.edu, humayun@magnet.fsu.edu), [2]Department of Earth Sciences, Carleton University, 1125 Colonel By Drive, Ottawa,
Ontario, Canada K1S5B6.

Introduction: Nucleosynthetic isotope anomalies in meteorites are reported in various meteoritic samples suggesting differences in incorporation of an isotopically diverse presolar dust [1-7]. Iron meteorites as planetary cores formed by magmatic fractionation are recording such anomalies and they have been reported on Ru, Mo, W, but apparently not resolved in Os [1-8] indicating systematic s-deficits and/or r-process excesses on a planetary scale. Such nucleosynthetic anomalies can be obscured like in Os or Pt isotopes [1] by cosmogenic effects (galactic cosmic ray GCR neutron capture) due to burning of isotopes with large thermal neutron cross sections (σ_γ) e.g. ^{191}Ir (effect on ^{192}Pt), ^{182}W, ^{189}Os, and ^{103}Rh (^{104}Pd). An excess of CAIs (refractory element enrichment) which record endemic nucleosynthetic anomalies [9] in protoplanets can induce s-processes deficiencies for refractory elements (Mo, Ru, W, and Os) in iron meteorites. But such effects should not be visible in non-refractory elements. Therefore, Pd isotopic compositions provide a critical constraint on the underlying causes of nucleosynthetic isotope anomalies in differentiated meteorites.

The isotopic compositions of many key geochronometers, particularly ^{182}W, but also ^{187}Os, require significant corrections for cosmogenic neutron capture. This is best achieved by use of an in situ neutron dosimeter (e.g., [1, 10]). The correlation between the isotopic shift on the neutron dosimeter and that of the geochronometer of interest are dependent on the position of the high-energy neutron capture resonances for both isotopes since cosmogenic neutrons are not significantly thermalized before they diffuse out of metre-sized irons [11]. Therefore, it is essential to explore additional neutron dosimeters besides those based on ^{189}Os(n,γ)190Os [1, 8] and ^{191}Ir(n,γ, β^-)^{192}Pt. In this regard, the reaction ^{103}Rh(n,γ, β^-)^{104}Pd has considerable potential due to the high neutron capture cross-section of ^{103}Rh [14, 11]. With high-precision isotope measurements of 104Pd it is now possible to resolve the cosmogenic effects [2].

We present new Pd isotopic compositions on IVB iron meteorites, the group of magmatic iron meteorites exhibiting the largest nucleosynthetic and cosmogenic isotope effects. During magmatic fractionation Pd (siderophile) partitions into the planetismal core but in contrast to other siderophile refractory elements (Mo, Ru, W, Os, Pt) Pd is not refractory [12]. Palladium has six isotopes with the p-only ^{102}Pd, s-only ^{104}Pd, r-dominated ^{110}Pd, in addition to ^{105}Pd, ^{106}Pd and ^{108}Pd that are formed by mixed s- and r-processes [13]. Due to the relatively high neutron cross section of ^{103}Rh [14] in this mass region GCR burning can result in accumulation of ^{104}Pd and therefore it can be used as in-situ dosimeter as shown in [2]. Possible nucleosynthetic anomalies (s-deficit and/or r-excess) result in negative ε^{104}Pd and positive ε^{110}Pd (Fig. 1) [13]. In the previous study [2], the deficits of ^{104}Pd were resolved but isobaric interferences on ^{110}Pd prevented a full confirmation. In this study, we report new Pd isotope data with both ^{104}Pd and ^{110}Pd anomalies.

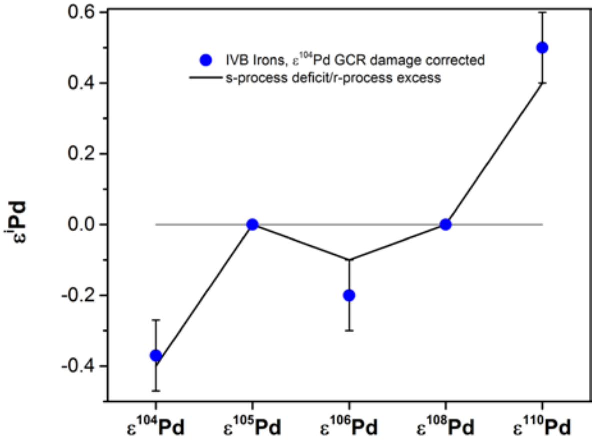

Fig. 1. Deficit/excess in s-or r-process for Pd to terrestrial standards using s-, p-, and r-process abundances from [13] scaled to an ε^{104}Pd=-0.4. GCR model from [11].

Analytical Methodology: Chemical separation procedures of Pd are similar to [1,2] but Pd was collected in HCl instead of HNO_3. Pd cuts from [2] which have shown interferences of Mo, Zn, and Zr have been reprocessed with this technique. The iron matrix is sufficiently removed by cation and anion exchange column chemistry as well as possible interferences (Mo, Ru, Cd, Zr, Zn, Yb, Ga, and Pt etc.). Pd isotope measurements were made during two sessions on the Thermo Neptune™ MC-ICP-MS (at the NHMFL, Tallahassee) in 100 ng/mL aliquots in 2% HCl with an ESI Apex™ introduction system and in 1µg/mL aliquots with an ESI SIS spray chamber introduction system in combination with Thermo SuperJet8.3 Ni sampler and Spectron T1001Ni-X skimmer cones. The Pd data are normalized to ^{108}Pd/^{105}Pd (1.18899) [15] using the exponential law for mass bias correction. We report data as ε^{104}Pd and ε^{110}Pd using as terrestrial bracketing reference material ICP-MS Pd standard Alfa Aesar (100ng/µl, 1µg/ml, respectively, n=240). Typical within-session external reproducibility for ε^{104}Pd and ε^{110}Pd is 0.1ε and 0.07ε, respectively. During this study we were able to remove the previously reported interferences in some sample cuts on mass 110 and 106 due to a final removal of Zr. Isobaric Ru and Cd interferences were negligible or correctable due to monitoring of ^{101}Ru and ^{111}Cd as tested with a standard. Possible molecular interferences from Zr, Zn and Ni, etc., were monitored prior to Neptune analysis using a Thermo Element2^{TM}).

Results: Distinct isotopic anomalies are resolved for the new Pd cuts, as well as the old cuts [2], showing ε^{104}Pd and ε^{110}Pd deviation from terrestrial Pd standard (Alfa Aesar). ε^{104}Pd shows a spread from -0.2 εu for Skookum, Tinnie, Warburton Range to 0.0 εu (Dumont) to 0.3 εu (Iquique) and 0.9 εu for Tlacotepec and is well correlated with ε^{192}Pt (Fig 2). Isotopic anomalies of IVB meteorites in ε^{110}Pd range from 0.4 to 0.6±0.1 εu. Only in one sample (Dumont) a negative ε^{106}Pd anomaly could be resolved with -0.2±0.1εu. The initial ε^{104}Pd of the IVB iron meteorites is distinctly negative at -0.37±0.02 within good agreement to previous results from this laboratory [2].

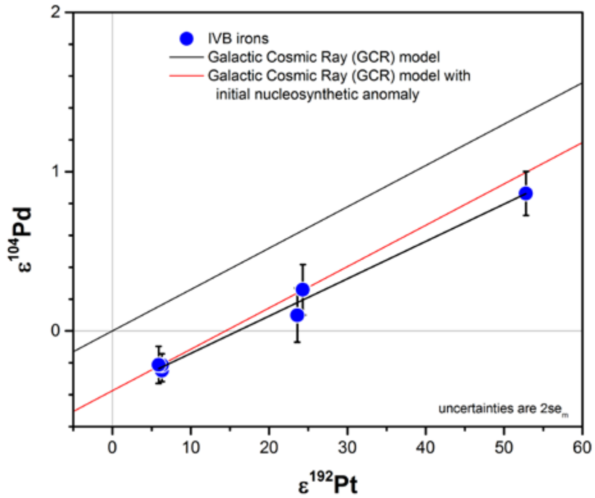

Fig. 2. ε^{192}Pt vs. ε^{104}Pd for IVBs with linear regression showing initial ε^{104}Pd of -0.37. In addition a GCR neutron capture model using paramters as in [1,11] and same model with this initial ε^{104}Pd anomaly is shown.

Discussion: Since neutron capture cross sections of Mo and Ru are small relative to ^{103}Rh GCR damage on those isotopes is negligible [3,4,14]. Thus, in this mass region the first signature of GCR damage is prone to be in an elevated ^{104}Pd. Comparing the ε^{104}Pd with the well understood in-situ dosimeter of ε^{192}Pd (due to burning of ^{191}Ir) shows a good correlation highlighting the ubiquitous secondary neutron capture reactions recorded in IVB irons, which obscure initial nucleosynthetic isotope anomalies in Pd. Regression of the correlation between ε^{192}Pt and ε^{104}Pd yields an ε^{104}Pd of -0.37±0.02 for IVB irons. This negative anomaly is in good agreement with predicted deficits due to s-process deficits and/or r-process excess [13] if Pd isotopes record the same deficits/excess observed in Mo and Ru for the IVB meteorites [3,4]. We predict a corresponding positive anomaly in the ε^{110}Pd of +0.4 εu (Fig 1). The measured anomaly is 0.5±0.1εu for the IVB iron meteorites which is in agreement with an s-deficit/r-excess. The negative (-0.2) ε^{106}Pd in Dumont can be attributed to s-process deficit/r-process excess (Fig. 1).

Carbon-rich condensates (SiC) are known to be carriers of nucleosynthetic anomalies in Mo and Ru and variations in SiC distribution in the nebula have been proposed as the causes of nucleosynthetic anomalies in iron meteorites [16, 17]. Since Pd is not known to form carbides, but ε^{104}Pd and ε^{110}Pd exhibit a well-resolved nucleosynthetic anomaly (s-process deficit/r-process excess) this makes variations in the distribution of SiC unlikely as the origin of these anomalies in IVB iron meteorites.

References: [1] Wittig, N. et al. (2013) EPSL, 361, 152-161. [2] Wittig, N. et al. (2013) 44rd LPSC, #2355. [3] Burkhard, C. et al. (2011) EPSL, 312, 390-400. [4] Chen, N. et al. (2010) GCA, 74, 3815-3862. [5] Fischer-Gödde, M. et al. (2012) 43rd LPSC, #2492. [6] Markowski, A. et al. (2006) EPSL, 250, 104–115. [7] Markowski, A. et al. (2006) EPSL, 242, 1-15. [8] Walker, R.J. (2012) EPSL, 315-352,36-44. [9] Brennecka, G. et al. (2012) 43rd LPSC, #2006. [10] Kruijer T. et al. (2013) EPSL 361, 162-172. [11] Leya I. and Masarik J. (2013) MAPS, 48, 665-685. [12] Lodders, K. (2003) APS, 591, 1220. [13] Arlandini, C. et al. (1999) APS, 525, 886-900. [14] Mughabhab, S.F. (2013) IAEA, 1-31. [15] Kelly, W. & Wasserburg, G. (1978) GRL, 5, 1079-1082. [16] Nicolussi, G. et al. (1998) Astrophys J, 504,492-499. [17] Dauphas, N. et al. (2004) EPSL, 226, 465-475.